Distributed e-fuel hubs: Concept and case study

Samy Mokeddem[a], Bardhyl Miftari[a], Victor Dachet[a], Guillaume Derval[a], Damien Ernst[a]

[a] *University of Liège, Smart Grids labs,*

Abstract

This paper introduces the concept of Distributed E-Fuel Hubs (DEFHs), which are small units, highly integrated in their environment and distributed across an area for local e-fuel production. In particular, they aim to take full advantage of local commodities such as unused by-products of local industries or local renewable energy. They can also benefit from local market opportunities, for example, by selling by-products of e-fuel synthesis, such as waste heat, through district heating networks. In addition, because of their distributed nature, DEFHs can reduce transportation costs by being located close to energy demand centers.

We assess the e-fuel production cost of this concept through a techno-economic analysis involving a DEFH synthesizing Fischer–Tropsch liquids, located near a lime plant in Belgium. Our analysis is based on a Linear Programming (LP) model for system sizing and operation planning, using hourly resolution data over one year. We consider a range of scenarios, from a low integrated DEFH with minimal local commodities integration and no by-products valorization, to a highly integrated scenario where the DEFH takes full advantage of local commodities and valorizes all of its by-products. These various scenarios highlight the impact of integration on e-fuel production cost. Our results show that DEFH integration can significantly reduce e-fuel production costs, achieving up to a 45% cost reduction in the highly integrated scenario compared to the low-integrated one.

Keywords: Energy-System, Power-to-X, E-fuel, Renewable Energy

1. Introduction

Global energy demand is growing, and at the same time, the amount of CO_2 emitted to meet that demand is rising. In the context of global warming, this upward trend in CO_2 emissions is concerning. The European Union has set itself the goal of a net-zero greenhouse gas (GHG) future (European-Commision, 2024b). To achieve this ambitious goal, all sectors must decarbonize their activities as much as possible. This fosters the need for finding new carbon-neutral ways to meet this energy demand.

Some sectors are inherently difficult to decarbonize due to their need for High Temperature (HT) heat and/or high-density energy storage. Sectors for which HT heat is crucial include, for instance, steel and cement production. These often require temperatures up to 1600°C, typically achieved through fossil fuel combustion (GROSS, 2021). Additionally, some sectors depend on certain production processes that emit CO_2 as a byproduct of chemical reactions. For example, the fundamental reaction of cement production involves the decomposition reaction of Calcium carbonate ($CaCO_3$) into calcium oxide (CaO) and CO_2. This chemical reaction accounts for 60% on average of the CO_2 emissions of the cement industry (GROSS, 2021). Other sectors, mostly related to long-haul transport, such as aviation and maritime transport, require energy-dense storage to cover long distances. Current commercial batteries lack sufficient energy density to power planes, ships, or long-haul trucks, leading these sectors to rely heavily on fossil fuels (GROSS, 2020). Consequently, both industrial and transport sectors face significant challenges in reducing their carbon footprint. These challenges are accentuated by the fact that, according to the European Parliament (European Parliament, 2024), the top 3 emitting sectors in 2022 are energy supply (27.4%), domestic transport (23.8%), and industry (20.3%).

In order to decarbonize these sectors, a number of solutions have been tried out. First, regarding the chemical reaction that produces CO_2 as a by-product, some works explored new possible reactions that release less CO_2

(Gartner, 2004; Bosoaga et al., 2009). However, there is no guarantee that such reactions can be developed, and even if they are discovered, implementing them may require transforming the entire production chain. This could result in high costs to replace or transform all production lines involved.

Secondly, regarding the fossil fuel usage for its properties (e.g. HT heat and high-density energy storage), there exist alternative solutions. For HT heat production, an approach can be to replace them with electric fuel (e-fuels). E-fuels are energy-dense molecules synthesized using low-carbon electricity. The simplest e-fuel to synthesize is green hydrogen (H_2), which releases no CO_2 during its production and combustion. However, its integration requires important investments to adapt existing facilities (International-Energy-Agency, 2019). To alleviate expensive facility modifications, a second approach can be to use hydrocarbon e-fuels. These e-fuels are synthesized by combining H_2 with CO_2. From a practical point of view, these hydrocarbon fuels have very similar properties to their fossil counterparts and can be used in the same applications. These e-fuels can be burned to produce HT heat. Moreover, these e-fuels have an energy density similar to that of fossil fuels. For instance, the aviation sector has shown great interest in e-kerosene due to its greenhouse gas (GHG) emission reduction targets (International-Air-Transport-Association, 2024). One simple solution is to convert the CO_2-rich flue gases emitted by the industries that inevitably produce it as a by-product into e-fuels that can then be used by sectors that require high-density energy storage. However, it should be noted that recycling CO_2 emitted into e-fuel only extends the life cycle of the CO_2 molecule before being released into the atmosphere, resulting in a lower but not neutral carbon footprint. Moreover, this extended life cycle idea can be extended beyond CO_2-rich flue gases.

In this paper, we introduce the concept of Distributed e-Fuel Hubs (DEFHs) that valorize local commodities and infrastructure to produce e-fuels. DEFHs are small units distributed across an area for local e-fuel production. To minimize their e-fuel production costs, these hubs aim to be strategically located and sized to take full advantage of the local infrastructure and local commodities, such as by-products from nearby industries (e.g. CO_2 in flue gases or waste heat) and renewable energies. Moreover, DEFHs can valorize the e-fuel synthesis by-products, such as oxygen or waste heat, in the local markets (e.g. selling waste heat for district heating). Finally, DEFH can reduce transport costs by being located near Energy Demand Centers (EDCs).

These EDCs can be airports for plane refueling, ports for ship refueling, or heavy industries that require e-fuels for HT processes.

The main advantage of these distributed hubs is their great emphasis on the local supply chain and production. Most European countries heavily depend on foreign countries for their fossil fuel supplies. That dependency on other countries can weaken their position in the case of geopolitical tension and reduce their ability to control energy costs. By installing DEFHs within their borders, countries can increase their energy sovereignty. Moreover, by installing multiple smaller e-fuel hubs over a centralized bigger unit, we can improve the supply chain's resilience. Indeed, in the case of an extreme event (e.g. earthquake, tsunami, bombing, etc.) impacting a DEFH, only a small proportion of the supply is lost. Conversely, in the case of an extreme event impacting a bigger centralized unit of production, the entire supply can be lost, and can lead to undesirable scenarios like forced shutdowns.

DEFH can also participate in other markets like the European (EU) Emission Trading System (ETS) and the service-to-grid markets. The EU ETS is a cap-and-trade mechanism designed to reduce GHG (e.g. CO_2) emissions by setting a limit on total emissions from certain sectors and allowing companies to trade emission allowances within this cap, aiming to incentivize the reduction of GHG in the target sector. DEFH installed within the EU can receive remuneration for helping industries to offset or avoid CO_2 emissions that exceed their allocated cap. The service-to-grid markets include the reserve electricity market, such as the Frequency Containment Reserve (FCR). The DEFH can help stabilize the local electrical grid by adapting its electricity consumption from the grid. This ancillary service can be a potential by-product of DEFHs as envisioned for electrolyzers in (Johnsen et al., 2023). This participation in these two potential markets can generate additional revenue streams that can reduce the production cost of DEFH.

There are barriers to DEFHs' deployment. The low quality of renewable resources in some European countries can increase e-fuels production costs. Additionally, DEFHs cannot benefit from economies of scale like larger centralized units, limiting their ability to optimize costs. To mitigate these two issues related to the production cost, DEFHs aims to be strategically located and sized to take full advantage of these three key factors: i)

the local commodities, such as by-products from nearby industries (e.g. fuel gas or waste heat) and renewable energy, ii) the local demand in a commodity that can be matched by e-fuel synthesis by-products (e.g., oxygen or waste heat), and iii) proximity to EDC to avoid costly transport logistics.

If the concept of DEFH is massively adopted, we can imagine a future in which almost every heavy industrial plant in the world would have its own DEFH that recycles the CO_2-rich flue gas produced by these plants into e-fuel. Consider, as an example, the cement industry to illustrate the potential impact of DEFHs. In 2022, the cement industry emitted around 4.3% CO_2 emissions worldwide (Hannah and Max, 2024). If these CO_2 emissions were captured and transformed into e-kerosene through a Fischer-Tropsch (FT) process, we could produce enough e-kerosene to fuel 66.42% of the commercial aviation fuel consumption in 2022, (International-Energy-Agency, 2024). This computation is detailed in Appendix C.1.

This paper introduces and formalizes the concept of Distributed E-Fuel Hubs (DEFHs), as detailed in Section 2. Section 3 illustrates the DEFH concept through various scenarios. Section 4 presented the methodology used to study these scenarios. The experiments associated with each scenario, along with their results, are presented in Section 5. The findings are discussed in light of the modeling assumptions in Section 6. The relevant literature is then reviewed in Section 7. Finally, this paper ends with a conclusion in Section 8.

2. DEFH Concept

In this section, the concept of a DEFH is presented and broken down into its principal components. The main idea behind the concept is to valorize the local commodities and infrastructure to produce e-fuel. The DEFHs are locally highly integrated units distributed across an area for local e-fuel production. To minimize their e-fuel production costs, these units aim to be sized and located to take full advantage of local infrastructures and commodities, such as by-products from nearby industries (e.g. CO_2 in flue gases or waste heat) and renewable energy that can be produced from different sources. Moreover, DEFHs are meant to valorize the e-fuel synthesis by-products, such as oxygen or waste heat, in locally unavailable markets (e.g. selling waste heat for district heating). Finally, DEFH can reduce transport costs by being located near EDCs. Although DEFHs can produce various e-fuels based on local demands, they share a common, generic structure.

This generic structure comprises three modules: the local opportunities, the e-fuel production, and the transport and markets. These modules are described in Subsection 2.1, Subsection 2.2, and Subsection 2.3, respectively. The generic DEFH structure is illustrated in Figure 1.

The subsequent section outlines the components of each module of a generic DEFH. The role of each component and the interaction between them are detailed.

2.1. Local opportunities module

The local opportunities module is the first module of the DEFH, responsible for extracting, converting, and transporting local commodities to the e-fuel production module. These local commodities include renewable energy sources as well as by-products from nearby industries. For instance, renewable energy may come from wind, solar, or geothermal energy, while industrial by-products can be CO_2-rich flue gases or waste heat. The local opportunities module also includes the exploitation of local infrastructure, such as the local high-voltage grid or gas network.

DEFH aims to produce low-carbon e-fuels, and an essential commodity in their production is low-carbon electricity. This low-carbon electricity can be produced by harvesting the local renewable energy potential and converting it into electricity through renewable energy plants. These renewable energy plants are installed according to the region's potential. For instance, a DEFH in southern Spain might rely on a renewable energy mix with a higher proportion of solar panels, capitalizing on the region's high solar energy potential. In contrast, a DEFH in Belgium might opt for an energy mix with more wind turbines, taking advantage of the region's windier but less sunny climate.

The DEFH concept also focuses on valorizing by-products of the nearby industries, such as waste heat or CO_2-rich flue gas, which can be reused in the e-fuel synthesis. For instance, these industries can be cement, lime plants, or any industry that is difficult to decarbonize due to the technical requirements of their production process. More precisely, one example is a lime plant that produces CO_2-rich flue gases that can be used as CO_2 sourcing if combined with a Post-Combustion Carbon Capture (PCCC) unit. This CO_2 sourcing can be advantageous in comparison with CO_2

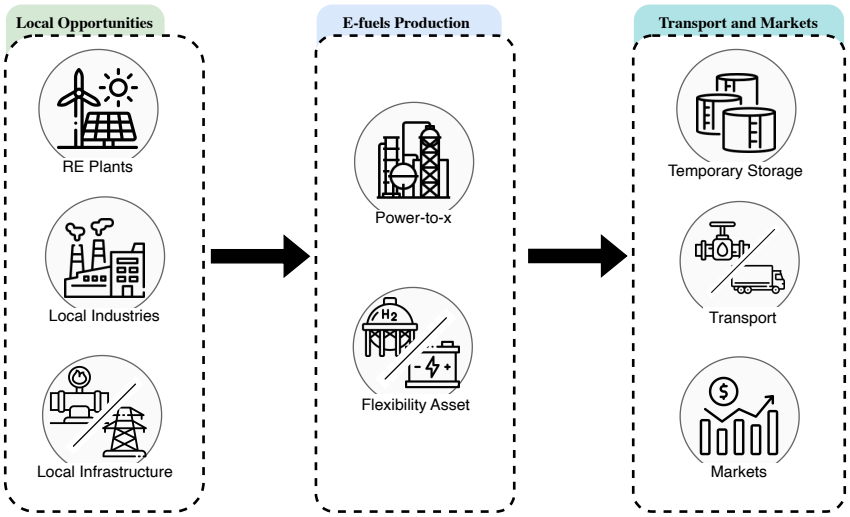

Figure 1: Concept diagram of a DEFH.

sourcing from Direct Air Capture (DAC), which is more energy-intensive (van der Giesen et al., 2017). Additionally, waste heat from nearby industries can be used to meet some of the heating demands for e-fuel synthesis.

2.2. *E-fuels production module*

The second module is the e-fuels production module. This module is responsible for combining and converting the input commodities into e-fuels. This process is often referred to as a power-to-x process.

The central asset in most e-fuels production is the electrolyzer. Electrolyzer decomposes the molecule of water (H_2O) into molecules of H_2 and dioxygen (O_2). This H_2 molecule can be directly used as an e-fuel but is often combined with other molecules to synthesize other e-fuels (e.g. e-methane or e-kerosene) that are easier to transport or/and compatible with actual fossil fuel distribution infrastructure or internal combustion engines. These electrolyzers use electricity as the energy source to enable this decomposition reaction, and if the electricity used in the process is low-carbon, the hydrogen produced is referred to as green hydrogen.

To produce more complex e-fuels, an important asset in e-fuels production is the feedstock capture asset. As said before, green H_2 can be combined with another molecule to synthesize e-fuel with similar properties to fossil fuel. This molecule, which is combined with H_2 is typically called a feedstock in e-fuel synthesis. The two most studied feedstocks are CO_2 and di-nitrogen (N_2). CO_2 can be used for the synthesis of hydrocarbons, while N_2 is commonly used for the production of ammonia.

Then, after synthesizing H_2 and capturing a feedstock, we can use chemical reactors to combine H_2 with feedstocks such as CO_2 or N_2 to synthesize the target e-fuel through chemical processes. These processes enable the production of various e-fuels, including e-methane, e-kerosene, e-diesel, and e-ammonia.

In the case study of this work, we focus on the synthesis of FT liquids, a blend of hydrocarbons with a typical mass distribution of approximately 60% e-kerosene, 20% e-diesel, and 20% e-naphtha, according to the Danish-Energy-Agency (2024). This mass distribution is not fixed. It can be adjusted to favor specific hydrocarbons by tuning key reactor parameters, notably the choice of catalyst and reactor operating temperature. A more detailed description of FT reaction and other e-fuel synthesis processes can be found in Palys and Daoutidis (2022) and Dieterich et al. (2020).

The final assets in this e-fuel production module are the flexibility assets, including electrical battery storage, H_2 storage, and CO_2 storage. These flexibility assets aim to manage the intermittency of renewable energy sources and the limited flexibility of other assets, such as the power-to-x reactor, which are not yet well understood under dynamic production loads Wentrup et al. (2022).

2.3. Transport and markets

The third and last module of the DEFH is the transport and markets module, which is responsible for delivering the synthesized e-fuels and their by-products to the end user and managing participation in markets.

The transportation part involves managing the flow of commodities to end users and markets, which can be achieved through various technologies. For instance, synthesized e-fuels can be transported via pipelines or trucks. In the case of truck transport or other discontinuous transport methods, temporary storage is necessary to manage the interval between truck arrivals at the production site. Additionally, trucks themselves can be powered by the e-fuels produced by the DEFH.

Moreover, valuable by-products generated during e-fuel synthesis, such as waste heat and oxygen from electrolyzers, can also be delivered to end users. For example, waste heat can be integrated into a local district heating system.

This last module also includes the markets in which DEFH can participate to generate additional revenue streams, along with the sale of e-fuels and by-products. Two particularly interesting markets for DEFH are the European Union Emission Trading System (EU ETS) and the service-to-grid markets.

Emission Trading System (ETS), like the EU ETS (European-Commision, 2024a) also called the European CO_2 market, is a cap-and-trade mechanism designed to reduce GHG (e.g. CO_2) emissions by setting a limit on total emissions from certain sectors and allowing companies to trade emission allowances within this cap, aiming to incentivize the reduction of GHG in the target sector. DEFHs installed within the EU can receive remuneration for helping industries to offset or avoid CO_2 emissions that exceed their allocated cap. When sourcing CO_2 from DAC, the DEFH offsets emissions, while sourcing CO_2 from PCCC avoids emissions. In both cases, the DEFH can be remunerated at the market emission allowance price for each ton of CO_2 converted into e-fuel.

The service-to-grid markets include the reserve electricity market, such as the Frequency Containment Reserve (FCR). The DEFH can help stabilize the local electrical grid by adapting its electricity consumption from the grid. This ancillary service can be a potential by-product of DEFHs as envisioned for electrolyzers in Johnsen et al. (2023).

This participation in these two potential markets can generate additional revenue streams that can reduce the production cost of DEFH.

3. DEFH instantiation

This section presents a techno-economic analysis of five DEFH scenarios with varying levels of local integration. The objective is to evaluate how integration strategies, such as access to local commodities and by-product valorization, can affect e-fuel production costs. The scenarios range from a minimally integrated DEFH with no by-product utilization to a highly integrated DEFH that takes full advantage of local commodities and valorizes all of its by-products.

The various scenarios considered are defined below. Additionally, a summary of all the scenarios is provided in Table 1.

Scenario	S1	S2	S3	S4	S5
District heating	×	×	×	×	✓
Oxygen Valorized	×	×	×	✓	✓
ETS	×	×	✓	✓	✓
CO_2 Sourcing	PCCC	DAC	PCCC	PCCC	PCCC

Table 1: Summary table of scenarios and their parameters.

Scenario 1: PCCC
For the baseline scenario, we considered a Belgian industrial site near the city of Namur with a lime plant emitting around 10 tons of CO_2 per hour. The DEFH is assumed to be installed in this industrial site and capture the CO_2 from the rich CO_2 flue gases to synthesize Fischer-Tropsch (FT) liquids. A schematic representation of the case study DEFH is shown in Figure 2.

For this base scenario, we considered that renewable electricity is harvested from solar and wind resources using photovoltaic (PV) panels and onshore wind turbines, respectively. Two types of PV systems are considered: fixed-mounted panels and tracking solar panels, which follow the sun's trajectory to improve energy yield. Moreover, we assume the local High-Voltage (HV) grid (i.e., the Belgian HV grid) is connected to the DEFH and used for electricity supply.

In this scenario and all the other scenarios, we consider DEFH synthesizing only FT liquids for the sake

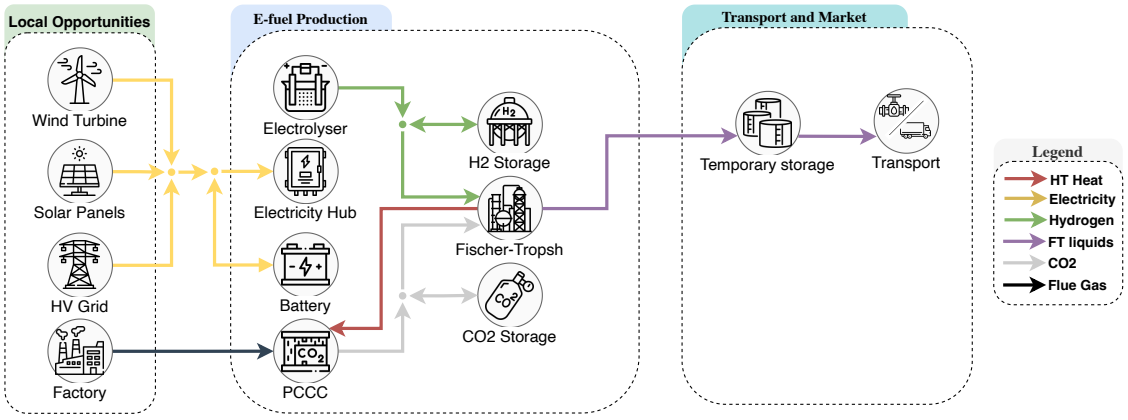

Figure 2: Diagram of the key component of the case study's DEFH Scenario 1. In this scenario, the revenues are solely generated from the selling of e-fuel, and CO_2 is sourced from PCCC. The "Electricity Hub" is an abstract connection point to which each component is considered to have access. For clarity, individual electricity connections are not drawn.

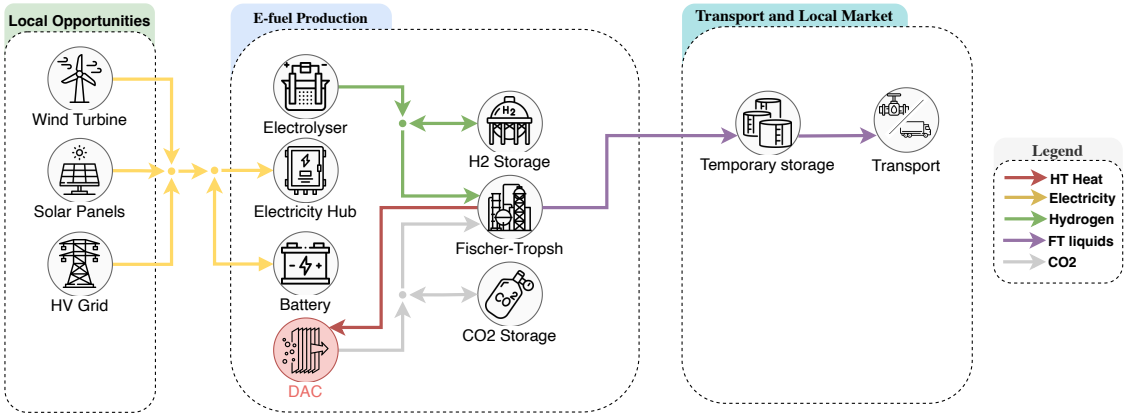

Figure 3: Diagram of the key component of the case study's DEFH Scenario 2. In this scenario the revenues are generated from the selling of e-fuel and CO_2 is sourced from DAC. The "Electricity Hub" is an abstract connection point to which each component is considered to have access. For clarity, individual electricity connections are not drawn.

of comparison. FT liquids are produced by combining H_2 and CO_2 in an FT reactor. First, H_2 is generated via water electrolysis. In this study, we consider the two most mature electrolyzer technologies: the Alkaline Electrolyzer Cell (AEC) and the Proton Exchange Membrane Electrolyzer Cell (PEMEC). Second, CO_2 is captured from the rich flue gas emitted by the co-located lime plant using a PCCC unit. Then, the captured CO_2 and produced H_2 are fed into an FT reactor to synthesize FT liquids.

As shown in Figure 2, the system includes electrical battery storage to manage the intermittency of renewable energy sources. In addition, H_2 and CO_2 storage units can be installed to increase system flexibility. In this instantiation, we also assume that a portion of the HT heat generated by the exothermic Fischer–Tropsch (FT) reaction is recoverable and used to partially meet the heat demand of the post-combustion carbon capture (PCCC) unit.

In this scenario, revenue is solely generated from the sale of the synthesized e-fuel. Moreover, in all scenarios, we do not model the transport part of the e-fuel, as the costs associated are dependent on the final user.

Scenario 2: DAC

The only difference with respect to Scenario 1 comes from CO_2 sourcing from DAC. In this scenario, the DEFH cannot take advantage of other local commodities, except for renewable energy, and does not valorize by-products. This scenario aims to identify the e-fuel

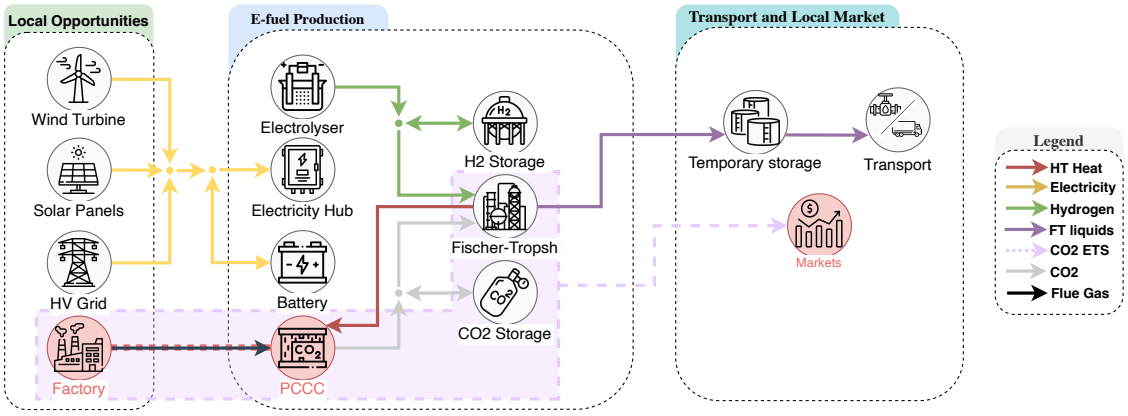

Figure 4: Diagram of the key component of the case study's DEFH Scenario 3. In this scenario the revenues are generated from the selling of e-fuel and ETS market participation, with CO_2 sourced from PCCC. The "Electricity Hub" is an abstract connection point to which each component is considered to have access. For clarity, individual electricity connections are not drawn.

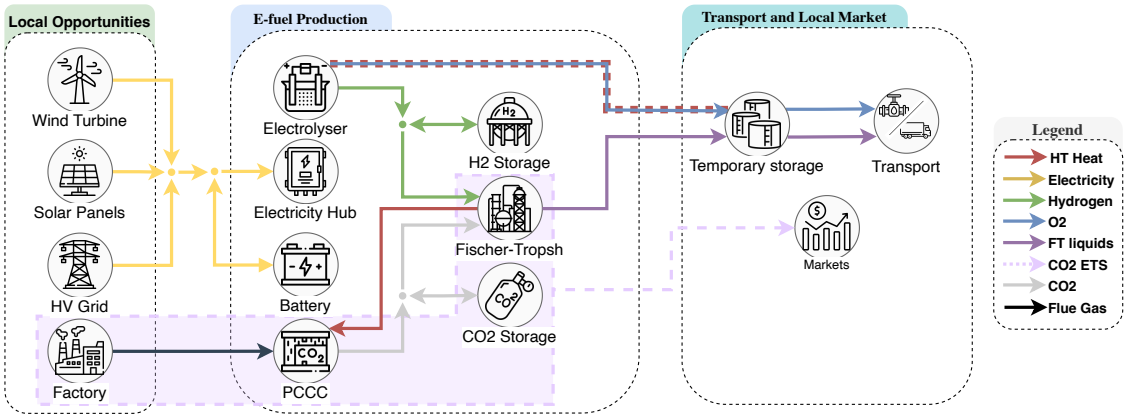

Figure 5: Diagram of the key component of the case study's DEFH Scenario 4. In this scenario the revenues are generated from the selling of e-fuel, ETS market participation and oxygen valorization with CO_2 sourced from PCCC. The "Electricity Hub" is an abstract connection point to which each component is considered to have access. For clarity, individual electricity connections are not drawn.

production cost when the DEFH is low-integrated. In this scenario, DAC ensures CO_2 sourcing, and revenue is solely generated from the sale of the synthesized e-fuel. Moreover, for the sake of comparison, we consider that the CO_2 capture rate is limited to the quantity of CO_2 capturable from the flue gases of the lime plant in the first scenario. A schematic representation of this scenario is shown in Figure 3.

Scenario 3: PCCC with ETS

This scenario is the same as the previous one, but we consider that the DEFH helps local industries that participate in the EU ETS market and is remunerated at the CO_2 emission allowance market price for each ton of CO_2 converted into e-fuel. We assume that the price of emission allowances is set at 80€ per CO_2 ton. However, the EU ETS market is an auction market, so the prices fluctuate over time, and this price uncertainty is studied in experiment 3 (more details can be found in 5.3). This scenario aims to assess the potential benefits of integrating the DEFH in such a market. A schematic representation of this scenario is shown in Figure 4.

Scenario 4: PCCC with ETS and valorization of O_2

This scenario mirrors the previous one but considers a DEFH that valorizes oxygen synthesized during electrolysis by selling it to local industries, for example. This scenario aims to determine the gains from oxygen valorization for the DEFH. In this work, we assume a price of €40 per tonne of oxygen, which is a lower estimation of the selling cost. Indeed, according to Breyer et al. (2015), the price can be up to €80 per tonne. A

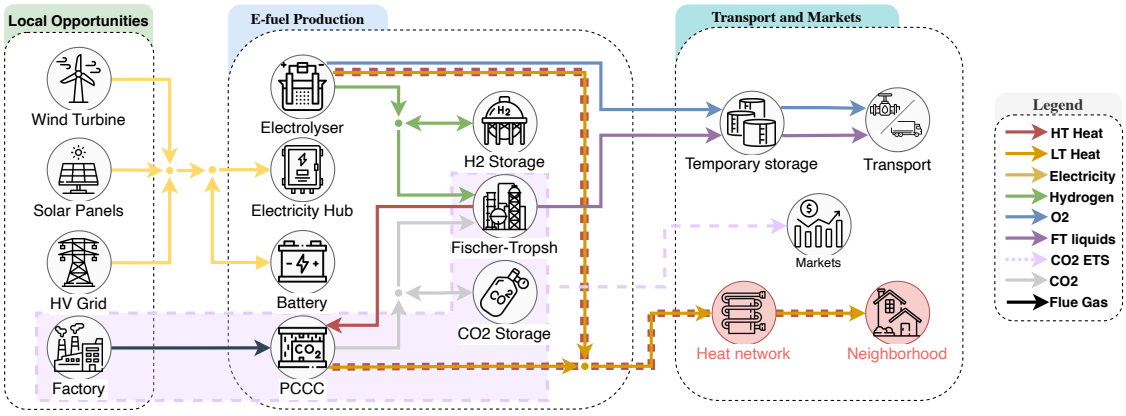

Figure 6: Diagram of the key component of the case study's DEFH Scenario 5. In this scenario, the revenues are generated from the selling of e-fuel, ETS market participation, oxygen and waste heat valorization with CO_2 sourced from PCCC. The "Electricity Hub" is an abstract connection point to which each component is considered to have access. For clarity, individual electricity connections are not drawn.

schematic representation of this scenario is shown in Figure 5.

Scenario 5: PCCC with ETS, valorization of O_2, and district heating
This last scenario showcases a highly integrated DEFH by adding the valorization of the waste heat to the previous scenario. This waste heat is considered to be sold as district heating through a local heat network. A schematic representation of this scenario is shown in Figure 6.

4. Methodology

To evaluate the impact of local integration on the e-fuel production cost, techno-economic analyses are performed over the different scenarios defined previously, ranging from a low-integrated DEFH to a highly integrated DEFH.

We model our DEFH instances as a linear program (LP). This LP model optimizes the asset's capacities and operations of the DEFH according to the local commodities (e.g. solar energy or wind energy) and the economic parameters (e.g. selling price of e-fuel by-products). However, the financial parameters, such as the selling price of e-fuels, by-products, and CO_2 emission allowances, are inherently uncertain and can directly impact DEFH's profitability. In our experiments, we assess the impact of these uncertainties across all scenarios.

The experimental setup is divided into three parts. Firstly, we present the modeling assumptions. Next, we describe the framework used to model the various scenarios of DEFH instantiation. Finally, we outline the data sources.

4.1. Modeling assumptions

Here, we list and discuss the different modeling assumptions taken for our techno-economic analysis.

Investment and Operational Decisions. A single-year investment horizon is considered. Investment decisions are made at the start of the period, with assets becoming immediately available. Operational decisions are made on an hourly basis. Both investment and operational planning are executed simultaneously using the LP optimization model.

Hourly resolution. The model considers an hourly resolution to capture both daily and seasonal variations in weather that affect load factors of renewable energy sources. This resolution is a good trade-off between computational time and model accuracy.

Perfect Foresight and Knowledge. The LP model assumes perfect foresight and knowledge, meaning that future weather conditions, electricity market prices, and all technical and economic parameters are known with certainty. No uncertainty is considered in the model, except during sensitivity analysis.

Linearity. All assets in the model are represented using linear input-output relationships. Even assets with inherently nonlinear behaviors, such as battery storage and electrolyzers, are approximated with linear models. This simplification is made as we have large problems

with hundreds of variables, and the linearity is a good tradeoff between computation time and precision.

Grid Access. The DEFH is assumed to be a sufficiently large consumer to connect to Elia's 36 kV grid in Belgium. We assume that a 1 km long cable is necessary for connecting the DEFH to the 36 kV grid and that investment in a 125 MVA transformer is also needed. Network and transformer costs are based on Elia's published tariffs for 2027 Elia (2024).

Market Interaction. The DEFH will purchase electricity through the Belgian day-ahead market but is not authorized to sell electricity back to the market. This restriction is applied to prevent the model from installing batteries or renewable energy plants (e.g., photovoltaic or wind turbines) solely for energy trading. Given the perfect foresight of the optimizer, it could otherwise exploit market fluctuations to maximize profits through trading, which is not the intended focus of this study.

Hypothetical Local Industry. The study aims to illustrate the benefits of coupling a DEFH to a local industry. To avoid creating an overly specialized problem, a simplified model of a local industry is used. This industry is represented as having a constant flue gas flow with a steady CO2 concentration.

Unconstrained Land Surface. We assume no direct constraints on land usage. However, land usage is indirectly limited by the CO2 capture rate, which limits the annual e-fuel production. This annual limit, combined with the cost minimization, inherently restricts the capacity of installed assets and thus land usage. Although this assumption is optimistic and might be unrealistic in some cases, it enables the determination of the cost-optimal asset configuration and the necessary land surface to achieve it.

Flexibility of Assets. We assume that all assets satisfy ramp-up and ramp-down constraints between consecutive time steps, given the hourly resolution of the model. Therefore, no ramp-up or ramp-down constraints are integrated into the model. Moreover, the Fischer–Tropsch process is modeled as operating at a steady-state rate, as its dynamic behavior remains insufficiently characterized (Wentrup et al., 2022). Additionally, minimal load constraints are applied to the electrolyzers; further details can be found in Appendix B.

4.2. Model formulation

We model our case study as a linear programming (LP) problem with GBOML (Graph-Based Optimization Modeling Language) Miftari et al. (2023). GBOML is an open-source Python framework for representing and solving Mixed-Integer Linear Programs (MILPs) by exploiting their structural characteristics, modeled as hierarchical hypergraphs. The overall framework is similar to the ones of Mbenoun et al. (2025); Dachet et al. (2023), and so will not be detailed in this work. But the mathematical formulation of the new or adapted node is presented in Appendix B, and the asset parameters and cost are all coming from Danish-Energy-Agency (2024).

4.3. Data sources

Renewable energy. The load factors for the photovoltaic panels and the wind turbines is taken from the Renewables Ninja website, which is based on Staffell and Pfenninger (2016); Pfenninger and Staffell (2016).

Assets datasheet. The parameters and costs of the different assets are taken from the projections of the Danish Energy Agency's Technology Catalogues for the year 2030 (Danish-Energy-Agency, 2024).

Electricity costs. The electricity costs of the grid are based on the Day-ahead price in Belgium for the year 2023. These reference prices come from the ENTSO-E (2024).

5. Experiments

The five scenarios defined in the previous section consider different levels of local integration. These scenarios are subject to uncertainty on several economic parameters, namely the selling price of the e-fuels, the annual production, and the evolution of the market price of CO_2 emission allowances. To assess the impact of each of these parameters on these scenarios, we conduct three experimental analyses on each of these unknown parameters.

5.1. Experiment 1: Minimum e-fuel selling price

The first experiment aims to determine the minimum selling price of e-fuels at which the model begins to produce them for each scenario. This minimum selling price corresponds to the price at which producing e-fuels becomes profitable. This tipping point reflects the influence of local integration on production cost. We perform a sensitivity analysis by varying the e-fuel price

Inputs	S1	S2	S3	S4	S5
CO_2 tax [€/t]	0	0	80	80	80
O_2 price [€/t]	0	0	0	40	40
Heat price [€/MWh_{LHV}]	0	0	0	0	40
CO_2 sourcing	PCCC	DAC	PCCC	PCCC	PCCC
Results	S1	S2	S3	S4	S5
Annual production [MWh_{LHV}]	254912	226100	254909	254914	254914
price [€/MWh_{LHV}]	204 (-10.9%)	229 (ref)	185 (-19.2%)	172(-24.9%)	125 (-45.4%)
ETS revenues [€/MWh_{LHV}]	0	0	19	19	19
O2 revenues [€/MWh_{LHV}]	0	0	0	13	13
Heat revenues [€/MWh_{LHV}]	0	0	0	0	47

Table 2: Summary of the minimum profitable selling price of e-fuel across the study scenarios, including the associated economic parameters for each scenario. The percentages are calculated compared to the reference scenario (S2).

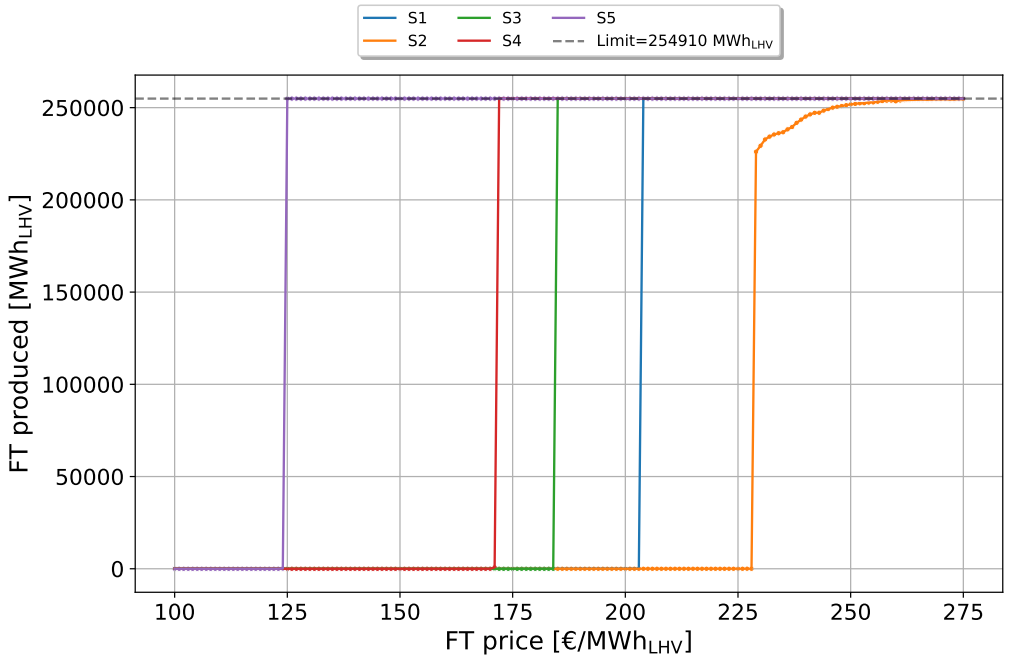

Figure 7: Sensitivity Analysis of the FT liquids production according to the FT liquids selling price.

from 140 €/MWh_{LHV} to 300 €/MWh_{LHV} in increments of 1€. For each price value, the LP model is solved to observe the resulting annual production. This analysis helps to identify the minimum profitable selling price under different integration levels.

The results show that the minimum profitable selling price of e-fuels varies across scenarios. Notably, scenarios with higher levels of local integration exhibit lower minimum profitable selling prices, highlighting the potential of integrated e-fuel production to reduce production costs. These results are presented in Table 2.

The results also show that sourcing CO_2 from DAC to PCCC has a noticeable impact on the minimum profitable selling price. The cost difference between DAC and PCCC can be attributed to two main factors. First, DAC requires more energy per ton of CO_2 captured compared to PCCC. Second, a significant portion of PCCC's energy needs can be supplied by the waste HT heat (around 200°C) generated during the FT synthesis reaction. However, this waste heat reuse is not feasible for DAC, as it requires very high temperature heat (around 900°C) to maintain its operating conditions. The results indicate that PCCC is less costly for CO_2 sourcing compared to DAC. However, PCCC requires that the DEFH be located close to industries emitting CO_2 or importing CO_2 captured with PCCC, which complicates the logistic chain and can increase the cost of the CO_2 ton.

By comparing the minimum profitable selling price of scenario one (S1) with scenario three (S3) in Table 2, we can see that the ETS can reduce the minimum profitable selling price by 19€. It represents around 8.3% of the minimum profitable selling price of the "DAC" scenario (S2). The decrease in minimum profitable selling price is attributed to the additional revenue generated from participating in the ETS market, alongside the sale of e-fuels and by-products. This additional revenue offsets a part of the production cost and, therefore, reduces the minimum profitable selling price.

The minimum profitable e-fuel selling price of scenario four (S4) is 13€/MWh_{LHV} lower than scenario three (S3). This is due to the sale of O_2, and this reduction corresponds to approximately 5.7% of the reference scenario (S2). Furthermore, waste heat valorization for district heating in scenario five (S5) results in the most significant cost reduction, lowering the minimum profitable selling price by 47€/MWh_{LHV} between S4 and S5. This reduction corresponds to 20.5% of the production cost of S2. Among all the integration strategies analyzed, waste heat valorization shows the highest impact on production cost. However, this result should be interpreted with caution, as the model assumes a fixed heat selling price and does not consider the infrastructure or operational costs associated with district heating networks. Nonetheless, additional analysis reveals a linear relationship between heat price and the minimum e-fuel selling price, with an approximate decrease of 1.18€/MWh for every 1€/MWh increase in heat price. This result can be attributed to the problem formulation as an LP problem and the energy ratio between Fischer–Tropsch liquid energy and recoverable district heating energy.

These results show that by-product valorization and market participation can help reduce e-fuel production costs. However, even in the highly integrated scenario (S5), the minimum profitable selling price remains at 125€/MWh_{LHV}, which is still significantly higher than the estimated market value of equivalent fossil-based Fischer–Tropsch liquids, approximated at 66€/MWh_{LHV} based on the petroleum fraction assumed in this work (see Appendix C.2 for details).

Figure 7 shows the production of e-fuel according to the e-fuel price. In all scenarios, the production curve exhibits a sharp discontinuity at the tipping point, increasing from zero to the theoretical maximal production for all the scenarios except the second (S2), which reaches a point close to the theoretical maximum. Beyond this point, production increases gradually toward the theoretical limit. This theoretical limit represents the maximum annual e-fuel production achievable based on the total capturable CO_2 over the year and the carbon efficiency of the synthesis process. The gap between production and the theoretical limit observed for S2 is caused by periods when production is not profitable due to either low availability of renewable energy or high electricity prices. As the selling price increases, such unprofitable production periods become less frequent.

Furthermore, CO_2 sourcing from DAC in S2 results in lower annual e-fuel production at the minimum profitable selling price compared to PCCC. This is primarily due to the higher energy demand of DAC, which increases reliance on the grid. As a result, electricity sourcing becomes more expensive, rendering more production periods economically unprofitable. To minimize production costs over the year, the model avoids producing e-fuel during these unprofitable periods, thereby reducing the overall annual production compared to scenarios with CO_2 sourcing from PCCC.

5.2. Experiment 2: Optimal annual e-fuel production

The second experiment investigates the optimal annual e-fuel production. To determine this, we assess how enforcing a minimum annual e-fuel production impacts the average cost of production. Similar to the first experiment, we performed a sensitivity analysis. We run several simulations, gradually increasing the minimum production from 19,900 MWh_{LHV} to 254,900 MWh_{LHV} (i.e. the theoretical production limit) in steps of 10,000 MWh_{LHV}. For each minimum production level, the LP model is solved to observe the resulting average price.

Results	S1	S2	S3	S4	S5
optimal production [MWh_{LHV}]	254900	228900	254900	254900	254900
minimum price [€/MWh_{LHV}]	204	229	185	172	125

Table 3: Summary of the minimum price of e-fuel across the study scenarios for experiment two.

As shown in Figure 8, the average cost curve demonstrates that costs decline with increasing production until reaching an optimal production point, beyond which the mean cost starts to rise. This first phase of cost reduction is primarily driven by the fixed connection costs to Elia's grid (Belgium's high-voltage network), which are amortized over higher production volumes. The increase after the optimal production point is attributed to the need to produce during less favorable periods, where electricity must be sourced at higher prices due to low renewable availability and high electricity market prices. Moreover, key results of these experiment are reported in Table 3

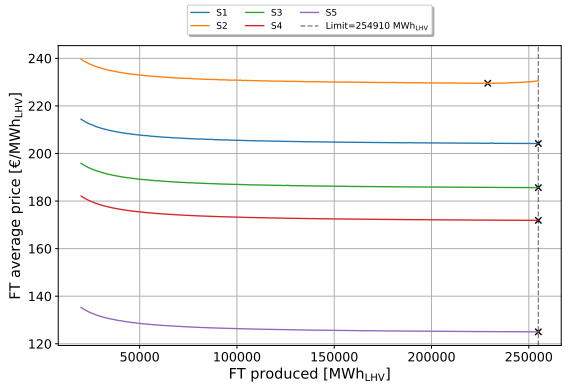

Figure 8: Sensitivity analysis of the FT liquids average production cost according to the FT liquids' yearly total production. The CO_2 emission allowance price is set at 80 €/t, and the price of oxygen at 40 €/t. The cross on each line represents the minimum price over the sensitivity analysis.

5.3. *Experiment 3: Impact of CO2 Emission Pricing*

The third and final experiment explores how regulatory measures, such as subsidies or CO_2 emission taxes, affect the profitability of e-fuel production. The impact is analyzed by studying the FT liquids production quantity regarding the CO_2 emission allowance price. As in the previous experiments, a sensitivity analysis was conducted across the relevant scenarios; scenarios S1 and S2 were excluded, as they do not participate in the EU ETS market. We run several simulations, gradually increasing the CO2 emission allowance price from 400€/tCO_2 to 800€/tCO_2 in steps of 5€. For this experiment, we have set the price of oxygen at 40€/t and the price of FT liquids at 66€/MWh_{LHV}. This price is based on the oil market price and the petroleum fraction considered for FT liquids. More details on this calculation can be found at Subsection Appendix C.2.

Table 4 shows that with the actual price of the FT liquids, the CO_2 emission allowance needs to be pushed around 400€ per ton to make the production of FT liquids profitable with a price of the district heating set at 40€ per MWh_{LHV}. The current price of the CO_2 emission allowance is around 80€ per ton and must increase five times to make the production of FT liquids with a DEFH in Belgium profitable. As shown in Figure 9, there is the same discontinuity as in 7 at the tipping points, which represent the minimum profitable CO_2 emission allowance price. Furthermore, in the lowest integrated scenario, production only becomes viable at a CO_2 price of 665€/ton, which is more than eight times the current price. These findings suggest that CO_2 taxes alone may not be sufficient to make e-fuels competitive, even in highly integrated e-fuel production settings. Additional factors, such as a willingness from certain stakeholders (e.g., the aviation sector) to pay a premium for low-carbon fuels over fossil fuels, may be necessary to enable the emergence of a low-carbon e-fuel supply. Once this supply is in place, it may benefit from economies of scale, similar to the cost reductions observed in the deployment of distributed renewable energy systems like solar panels.

Results	S3	S4	S5
price [€/tCO_2]	665	605	400

Table 4: Summary of the minimum profitable CO_2 emission allowance price across the study scenarios.

6. Limitations, future works, and comparison with literature

This study offers valuable insights, but several limitations should be noted. First, the use of linear approx-

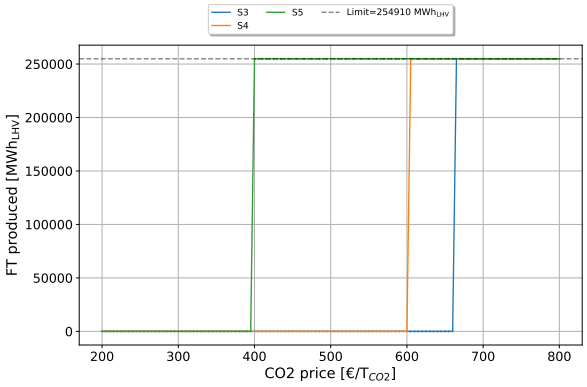

Figure 9: Sensitivity analysis of FT liquid production according to the CO_2 emission allowance price, with a price of FT liquids set at 55 €/MWh$_{LHV}$ and a price of oxygen at 40 €/t.

imations to model assets may not fully capture their complex behaviors, potentially leading to a gap with practical conditions. Second, assuming perfect foresight simplifies the analysis but may not account for real-world uncertainties in weather, market prices, and technical parameters. We also assume that the FT reactor cannot ramp up or down its production. The literature does not provide clear information on the ramping capabilities of such reactors. Relaxing this constraint could help to size these assets optimally given their ramping capabilities.

Additionally, our work considers a planning and control linear programming (LP) model for the year 2023 only. Extending this planning and control over a longer period or multiple historical periods could provide a better assessment of the results and production costs. Furthermore, the assumption of unconstrained land availability is optimistic and may not be practical, especially in densely populated or environmentally sensitive areas.

Future work could integrate grid ancillary service markets into the DEFH model, which could show economic benefits that can reduce the production price. Another direction for future work is to explore advancements in electrolyzers and carbon capture technologies, which could enhance the efficiency and, hence, decrease the production cost of DEFHs. Additionally, while this study focuses on a single case study in Belgium, analyzing other locations in the world can provide a broader assessment of DEFH production costs and feasibility. Another aspect that can make this local hub more competitive compared to RREH (i.e., importing energy) is the WACC. Indeed, a lower WACC implies lower production costs. The WACC could often be lower for plants installed in the EU than in foreign countries, such as Maghreb countries or Latin American countries.

To further contextualize our results, regarding the highly integrated scenario that presents the lowest production cost of 125€/MWh$_{LHV}$. This production cost falls within the cost range of Fasihi et al. (2017), which examines the production of low-carbon e-fuels in the Maghreb region through renewable energy plants, AEC electrolyzers, and DAC for CO_2 sourcing. Moreover, our production cost is a bit higher than Pfennig et al. (2023), which simulated production costs for various e-fuels, including FT liquids with RREH installed across the globe for import to Germany. This comparison indicates that e-fuel can be produced in Western Europe at competitive costs, provided that production is well-integrated into its environment and maximizes the valorization of local commodities, existing infrastructure, and e-fuel synthesis by-products.

7. Related work

The concept of Distributed E-Fuel Hubs (DEFHs) is encapsulated in the more generic energy hubs concept Geidl et al. (2007) and Sadeghi et al. (2019). The energy hub concept envisions production units using multiple commodities (e.g., gas, petrol, biomass) to produce various energy carriers (e.g., fuel, electricity, heat) to meet demand. Energy hubs aim to be resilient and efficient units able to produce multiple energy carriers. In this energy hub concept, a DEFH can be seen as an energy hub that produces low-carbon e-fuel from various local commodities into e-fuel and valorizes the e-fuel synthesis by-products to meet local demand, to minimize the marginal e-fuel production cost.

The DEFH concept focuses on three main components: i) production of low-carbon e-fuels, ii) the valorization of local by-products and existing infrastructure, and iii) the valorization of e-fuel synthesis by-products.

These concepts have already been studied independently in other works. Zeman and Keith (2008) was among the first to propose the production of low-carbon fuel using renewable energy plants and carbon capture technology to achieve carbon neutrality in hydrocarbon fuels. Additionally, Graves et al. (2011) was pioneering in quantifying the production cost of low-carbon fuel. These studies fall into the realm of DEFH even though they consider little to no valorization of by-products and infrastructure.

Daiyan et al. (2020) already highlighted the interest of integrating e-fuel production hubs into markets such as service-to-grid markets and/or CO_2 market, generating additional revenue streams, but does not quantify this potential revenue.

For by-product valorization, recent works explore the idea of valorizing waste heat or CO_2-rich flue gases from local industries. For instance, León et al. (2024) examined the cost of e-methanol production valorizing CO_2-rich flue gases of a cement plant, but did not highlight the cost reduction introduced by this valorization. Another study Koumparakis et al. (2025) explored the use of heat as a commodity flow within the hub, showing that reusing heat internally and externally can reduce e-fuel production costs. These articles can also be seen as instances of DEFH.

The concept of DEFH is also closely linked to the Remote Renewable Energy Hubs (RREH) concept (Berger et al., 2021; Dachet et al., 2025). RREHs are energy hubs that harvest renewable energy in regions where it is abundant or of high quality to export it. DEFH proposes an alternative approach, which is to produce locally e-fuel by taking full advantage of the unused by-products and existing infrastructure to minimize e-fuel production cost. DEFH wants to be a flexible solution, easy to deploy and integrate into an existing environment.

In summary, previous works have often focused on individual vectors of integration, and/or do not exhibit the cost reductions introduced by these integrations. In our work, we formalize the DEFH concept but also propose a case study that highlights the impact on e-fuel production cost of different vectors of integration. Specifically, we consider i) valorizing local by-products (e.g., CO_2-rich flue gases), ii) e-fuel synthesis by-products (e.g., waste heat), and iii) integration into regional markets (e.g., EU ETS market).

8. Conclusion

In this work, we introduced and formalized the concept of Distributed E-Fuel Hubs (DEFHs): small-scale, locally integrated units designed for decentralized e-fuel production. To minimize their e-fuel production costs, these units aim to be well integrated in their environment by being strategically sized and located to take full advantage of local commodities, opportunities, and proximity to Energy Demand Centers (EDCs).

In order to study this concept, this paper models a DEFH with various levels of integration so as to assess the integration's impact on the e-fuel production. More precisely, we conduct a techno-economic analysis of a DEFH configured for Fischer–Tropsch liquid synthesis in Belgium. The levels of integration range from a low-integrated DEFH with minimal local commodity integration and no by-product valorization, to a highly integrated DEFH where we take full advantage of local commodities and valorize all of the by-products. The results indicate that a higher level of integration reduces the minimum profitable selling price by around 45%, with 229€/MWh_{LHV} for the minimal integration DEFH and 125€/MWh_{LHV} for the highest level of integration. These results show the potential impact of integration on production cost.

The DEFH concept is complementary to other CO_2 emission reduction strategies, such as increasing low-carbon electricity production or electrifying fossil fuel-intensive sectors. Nevertheless, the DEFH concept represents more than only a technical concept. DEFHs offer a strategic pathway toward a resilient, low-carbon energy future. By taking advantage of existing industrial ecosystems, valorizing unused by-products, and participating in local markets, DEFHs can unlock synergies that centralized production models overlook. Their modularity, adaptability, and potential for rapid deployment make them particularly suited for accelerating the decarbonization of hard-to-abate sectors such as aviation and industry. With appropriate policy support and stakeholder engagement, DEFHs could become a cornerstone of future energy systems - empowering regions to produce clean fuels locally, reduce dependence on imports, and valorize local renewable resources.

CRediT authorship contribution statement

Samy Mokeddem: Writing - original draft, Methodology, Conceptualization, Software, Data Curation. **Bardhyl Miftari**: Writing – review & editing, Conceptualization. **Victor Dachet**: Writing – review & editing, Conceptualization. **Guillaume Derval**: Writing – review & editing. **Damien Ernst**: Writing – review & editing, Funding acquisition, Supervision.

Acknowledgments

The authors thank Antoine Larbanois for his feedback on the writing of this paper. They also thank Antoine Rouxhet for the insightful discussions on the technical workings of the Fischer–Tropsch process. Samy Mokeddem and Victor Dachet gratefully acknowledge the financial support of the Fonds de la Recherche Scientifique (FNRS). Moreover, Bardhyl Miftari gratefully acknowledges the financial support of the Public Service of Wallonia through the funding of the NKL project in the framework of the Recovery and Resilience Plan (PNRR), initiated and financed by the European Union.

Declaration of competing interest

The authors declare that they have no known competing financial interests or personal relationships that could have appeared to influence the work reported in this paper.

Data and code availability

The code and the date used in this study can be found here: DEFH repository (Mokeddem, 2025).

Declaration of Generative AI and AI-assisted technologies in the writing process

During the preparation of this work, the author(s) used ChatGPT and LeChat in order to correct the readability, grammar, and spelling of the writing. After using this tool/service, the authors reviewed and edited the content as needed and take full responsibility for the content of the publication.

References

Berger, M., Radu, D., Detienne, G., Deschuyteneer, T., Richel, A., Ernst, D., 2021. Remote renewable hubs for carbon-neutral synthetic fuel production. Frontiers in Energy Research 9. URL: https://www.frontiersin.org/journals/energy-research/articles/10.3389/fenrg.2021.671279, doi:10.3389/fenrg.2021.671279.

Bosoaga, A., Masek, O., Oakey, J.E., 2009. CO_2 capture technologies for cement industry. Energy Procedia 1, 133–140. URL: https://www.sciencedirect.com/science/article/pii/S1876610209000216, doi:https://doi.org/10.1016/j.egypro.2009.01.020. greenhouse Gas Control Technologies 9.

Breyer, C., Tsupari, E., Tikka, V., Vainikka, P., 2015. Power-to-gas as an emerging profitable business through creating an integrated value chain. Energy Procedia 73, 182–189. URL: https://www.sciencedirect.com/science/article/pii/S1876610215014368, doi:https://doi.org/10.1016/j.egypro.2015.07.668. 9th International Renewable Energy Storage Conference, IRES 2015.

Dachet, V., Benzerga, A., Coppitters, D., Contino, F., Fonteneau, R., Ernst, D., 2023. Towards CO_2 valorization in a multi-remote renewable energy hub framework. URL: http://dx.doi.org/10.52202/069564.

Dachet, V., Dubois, A., Miftari, B., Fonteneau, R., Ernst, D., 2025. Remote renewable energy hubs: A taxonomy. Energy Reports 13, 3112–3120. URL: https://www.sciencedirect.com/science/article/pii/S2352484725001258, doi:https://doi.org/10.1016/j.egyr.2025.02.040.

Daiyan, R., MacGill, I., Amal, R., 2020. Opportunities and challenges for renewable power-to-x. ACS Energy Letters 5, 3843–3847. URL: https://doi.org/10.1021/acsenergylett.0c02249.

Danish-Energy-Agency, 2024. Technology catalogues. URL: https://ens.dk/en/our-services/technology-catalogues. accessed: 2024-10-23.

Dieterich, V., Buttler, A., Hanel, A., Spliethoff, H., Fendt, S., 2020. Power-to-liquid via synthesis of methanol, DME or Fischer–Tropsch-fuels: a review. Energy & Environmental Science URL: https://api.semanticscholar.org/CorpusID:221681221.

Elia, 2024. Facturation et tarifs. URL: https://www.elia.be/fr/clients/facturation-et-tarifs. accessed: 2024-11-06.

EnergiaFed, 2025. Prix Maximums. https://www.energiafed.be/fr/prix-maximums. Consulté le 10 juin 2025.

ENTSO-E, 2024. Day-ahead prices for Belgium. https://transparency.entsoe.eu/transmission-domain/r2/dayAheadPrices/show?name=&defaultValue=false&viewType=TABLE&areaType=BZN&atch=false&dateTime.dateTime=01.12.2023+00:00|CET|DAY&biddingZone.values=CTY|10YBE----------2!BZN|10YBE----------2&resolution.values=PT60M&dateTime.timezone=CET_CEST&dateTime.timezone_input=CET+(UTC+1)+/+CEST+(UTC+2). Accessed: 2024-11-06.

European-Commision, 2024a. Eu ETS: EU emissions trading system. URL: https://climate.ec.europa.eu/eu-action/eu-emissions-trading-system-eu-ets_en. accessed: 2024-03-06.

European-Commision, 2024b. The european green deal: Striving to be the first climate-neutral continent. URL: https://commission.europa.eu/strategy-and-policy/priorities-2019-2024/european-green-deal_en. accessed: 2024-10-23.

European Parliament, E.P., 2024. Greenhouse gas emissions by country and sector (infographic). URL: https://www.europarl.e

uropa.eu/pdfs/news/expert/2018/3/story/20180301STO98928/20180301STO98928_en.pdf. accessed: 2024-11-06.

Fasihi, M., Bogdanov, D., Breyer, C., 2017. Long-term hydrocarbon trade options for the Maghreb region and europe—renewable energy based synthetic fuels for a net zero emissions world. Sustainability 9. URL: https://www.mdpi.com/2071-1050/9/2/306, doi:10.3390/su9020306.

Gartner, E., 2004. Industrially interesting approaches to "low-CO_2" cements. Cement and Concrete Research 34, 1489–1498. URL: https://www.sciencedirect.com/science/article/pii/S0008884604000468, doi:https://doi.org/10.1016/j.cemconres.2004.01.021. h. F. W. Taylor Commemorative Issue.

Geidl, M., Koeppel, G., Favre-Perrod, P., Klockl, B., Andersson, G., Frohlich, K., 2007. Energy hubs for the future. IEEE Power and Energy Magazine 5, 24–30. doi:10.1109/MPAE.2007.264850.

van der Giesen, C., Meinrenken, C.J., Kleijn, R., Sprecher, B., Lackner, K.S., Kramer, G.J., 2017. A life cycle assessment case study of coal-fired electricity generation with humidity swing direct air capture of CO_2 versus MEA-based postcombustion capture. Environmental Science & Technology 51, 1024–1034. URL: https://doi.org/10.1021/acs.est.6b05028. pMID: 27935700.

GlobalPetrolPrices.com, 2025. Belgique prix du kérosène. URL: https://fr.globalpetrolprices.com/Belgium/kerosene_prices/. consulté le 10 juin 2025.

Graves, C., Ebbesen, S.D., Mogensen, M., Lackner, K.S., 2011. Sustainable hydrocarbon fuels by recycling CO_2 and H_2O with renewable or nuclear energy. Renewable and Sustainable Energy Reviews 15, 1–23. URL: https://www.sciencedirect.com/science/article/pii/S1364032110001942, doi:https://doi.org/10.1016/j.rser.2010.07.014.

GROSS, S., 2020. The challenge of decarbonizing heavy transport.

GROSS, S., 2021. The challenge of decarbonizing heavy industry.

Hannah, R., Max, R., 2024. CO_2 emissions. URL: https://ourworldindata.org/co2-emissions. accessed: 2024-10-23.

International-Air-Transport-Association, 2024. Fly net zero - decarbonizing aviation. URL: https://www.iata.org/en/programs/sustainability/flynetzero/. accessed: 2024-09-20.

International-Energy-Agency, 2019. Transforming industry through CCUS.

International-Energy-Agency, 2024. Aviation - energy system. https://www.iea.org/energy-system/transport/aviation. Accessed: 2024-11-06.

Johnsen, A.G., Mitridati, L., Zarrilli, D., Kazempour, J., 2023. The value of ancillary services for electrolyzers. URL: https://arxiv.org/abs/2310.04321, arXiv:2310.04321.

Koumparakis, C., Kountouris, I., Bramstoft, R., 2025. Utilization of excess heat in future power-to-x energy hubs through sector-coupling. Applied Energy 377, 124098. URL: https://www.sciencedirect.com/science/article/pii/S0306261924014818, doi:https://doi.org/10.1016/j.apenergy.2024.124098.

León, D., Amez, I., Castells, B., Ortega, M.F., Bolonio, D., 2024. Techno-economic analysis of the production of synthetic fuels using CO_2 generated by the cement industry and green hydrogen. International Journal of Hydrogen Energy 80, 406–417. URL: https://www.sciencedirect.com/science/article/pii/S036031992402812X, doi:https://doi.org/10.1016/j.ijhydene.2024.07.138.

Mbenoun, J., Benzerga, A., Miftari, B., Detienne, G., Deschuyteneer, T., Vazquez, J., Derval, G., Ernst, D., 2025. Integration of offshore energy into national energy system: A case study on Belgium. Applied Energy 382, 125031. URL: https://www.sciencedirect.com/science/article/pii/S0306261924024152, doi:https://doi.org/10.1016/j.apenergy.2024.125031.

Miftari, B., Berger, M., Derval, G., Louveaux, Q., Ernst, D., 2023. Gboml: A structure-exploiting optimization modelling language in python. Optimization Methods and Software URL: https://gitlab.uliege.be/smart_grids/public/gboml, doi:10.1080/10556788.2023.2246169.

Mokeddem, S., 2025. DEFH repository. https://github.com/SamyMokeddem/DEFH. Accessed: 2025-08-13.

Palys, M.J., Daoutidis, P., 2022. Power-to-x: A review and perspective. Computers & Chemical Engineering 165, 107948. URL: https://www.sciencedirect.com/science/article/pii/S009813542200285X, doi:https://doi.org/10.1016/j.compchemeng.2022.107948.

Pfennig, M., Böttger, D., Häckner, B., Geiger, D., Zink, C., Bisevic, A., Jansen, L., 2023. Global GIS-based potential analysis and cost assessment of power-to-x fuels in 2050. Applied Energy 347, 121289. URL: https://www.sciencedirect.com/science/article/pii/S0306261923006530, doi:https://doi.org/10.1016/j.apenergy.2023.121289.

Pfenninger, S., Staffell, I., 2016. Long-term patterns of European PV output using 30 years of validated hourly reanalysis and satellite data. Energy 114, 1251–1265. URL: https://www.sciencedirect.com/science/article/pii/S0360544216311744, doi:https://doi.org/10.1016/j.energy.2016.08.060.

Sadeghi, H., Rashidinejad, M., Moeini-Aghtaie, M., Abdollahi, A., 2019. The energy hub: An extensive survey on the state-of-the-art. Applied Thermal Engineering 161, 114071. URL: https://www.sciencedirect.com/science/article/pii/S1359431117381851, doi:https://doi.org/10.1016/j.applthermaleng.2019.114071.

Staffell, I., Pfenninger, S., 2016. Using bias-corrected reanalysis to simulate current and future wind power output. Energy 114, 1224–1239. URL: https://www.sciencedirect.com/science/article/pii/S0360544216311811, doi:https://doi.org/10.1016/j.energy.2016.08.068.

Wentrup, J., Pesch, G.R., Thöming, J., 2022. Dynamic operation of Fischer-Tropsch reactors for power-to-liquid concepts: A review. Renewable and Sustainable Energy Reviews 162, 112454. URL: https://www.sciencedirect.com/science/article/pii/S1364032122003604, doi:https://doi.org/10.1016/j.rser.2022.112454.

Zeman, F.S., Keith, D.W., 2008. Carbon neutral hydrocarbons. Philosophical transactions Series A, Mathematical, physical, and engineering sciences. doi:https://doi.org/10.1098/rsta.2008.0143.

Scenario	S1	S2	S3	S4	S5
Wind Onshore [MW]	150.75	160.30	150.75	150.66	157.09
PV tracker [MW]	0	0.08	0	0	0
PV [MW]	125.56	131.19	125.56	125.42	125.58
Grid connection [MW]	125	125	125	125	125
CO2 tank [tCO_2]	0	271.44	0	0	0
CO2 liquefaction [tCO_2/h]	0	0.98	0	0	0
H2 tank [tH_2]	121.27	133.28	133.27	133.53	137.77
NaS Battery [MWh]	24.15	29.66	24.15	24.13	18.14
Li-ion Battery [MWh]	0	0.15	0	0	0
PEMEC [MW]	0	0.12	0	0	0
AEC [MW]	93.74	85.02	93.74	93.81	92.69
FT reactor [MW]	29.1	25.81	29.1	29.1	29.1
DAC [tCO_2/h]	0	9	0	0	0
PCC [tCO_2/h]	9	0	9	9	9

Table .5: Table showing the installed capacity of each asset at the minimum profitable selling price of Experiment 1, for each scenario.

Appendix A. Additional tables

In this section, we present the additional Table .5 that shows the assets' capacity installed by the model for each scenario at the minimum profitable selling price of Experiment 1 in Subsection 5.1.

Appendix B. Model Formulation

Appendix B.1. Notation

Before diving into the model formulation in the next section, we will define the notation used in this appendix.

Scalars are denoted by small letters a, α. Column vectors are denoted by small, bold letters $\mathbf{a}, \boldsymbol{\alpha}$.

Variables are always denoted by Roman letters $a, \mathbf{b}$, and parameters are always denoted by Greek letters $\alpha, \boldsymbol{\beta}$.

Appendix B.2. Model formulation

In this section, we formalize the DEFH presented in Section 3 as a linear programming problem.

First, let us define generic components that are then tuned to represent each specific technology. We model the DEFH as an hypergraph, which is a generalization of a graph in which a single edge, called a hyperedge, can connect several nodes. In our context, the nodes represent the assets (e.g., electrolyzers, solar panels, flexibility assets), while the hyperedges represent the flows of commodities (e.g., electricity, hydrogen, CO_2, heat) exchanged between these assets.

As stated previously in Subsection 4.2, this hypergraph is modeled using GBOML. Several nodes are the same as in Dachet et al. (2023); Mbenoun et al. (2025), and are therefore not detailed in this work. Their implementation is available in the project repository (link).

However, this section presents the mathematical formulation of newly introduced or modified nodes specific to our DEFH model. This includes, for instance, node adaptation with by-product valorization or the FT reactor node. Moreover, all the variables and parameters used in the following formalization are presented in Table B.6 and Table B.7.

Variable	Description	Unit
$\mathbf{q}_x^n$	Time-indexed vector of flow of commodity x in node n	depends of x (e.g. MWh or tons)
$\mathrm{k}_{x^*}^n$	Maximum flow (capacity) of reference commodity x^* in node n	depends on x^* (e.g. MWh or tons)
ψ_{spec}^n	Node-specific cost function	[€]
Parameter	**Description**	**Unit**
α_x^n	Conversion factor for input commodity x in node n	[–]
β_w^n	Conversion efficiency for output commodity w in node n	[–]
$\mu_{x^*}^n$	Minimum load factor for reference commodity x^* in node n	[–]
λ	Mean CO_2 flow from factory	[tons/h]
$\mathbf{1}$	Vector of ones of size T	[–]
$\eta_{co_2}^{FT}$	CO_2 conversion efficiency in FT reactor	[–]
$\boldsymbol{\phi}_x$	Time-indexed vector of selling price of commodity x	depends of x (e.g. €/MWh or €/tons)
Ω_{el}^G	Grid electricity capacity	[MW]

Table B.6: Summary of key variables and parameters used in the DEFH model formulation

Generic node. First, we will define the generic formulation of a node, which includes two main types of constraints: conversion constraints over the input and output flows and a set of flexibility constraints. These constraints aim to approximate the dynamics of the node.

A conversion constraint represents the conversion process from input commodities into output commodities and can be modeled as follows:

$$\alpha_x^n \mathbf{q}_\mathbf{x}^\mathbf{n} = \beta_\mathbf{w}^\mathbf{n} \mathbf{q}_\mathbf{w}^\mathbf{n}\,, \tag{B.1}$$

where $\mathbf{q}_x^n$ denotes a time-indexed vector of size T representing the flow of the commodity x in the node n at each time step $t \in [0, T-1]$. The parameter $\alpha_x^n \in [0,1]$ is the conversion factor of the commodity x in the node n, and $\beta_w^n \in [0,1]$ is the conversion efficiency into the commodity w in the node n. This generic node formulation is illustrated in Figure B.10

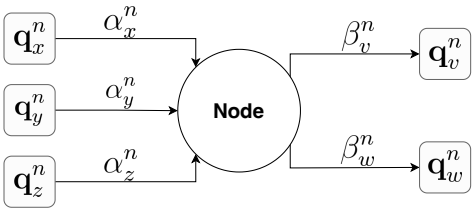

Figure B.10: Generic node representation.

Flexibility constraints include ramp-up, ramp-down, and load limits. In this work, as explained before in Section 4, we consider that ramp-up and ramp-down constraints are always satisfied between two time steps. Therefore, our model only has minimum and maximum load constraints. Each node is associated with a reference commodity, and the flow of this reference commodity is subject to these load limits. The constraints can be expressed as follows:

$$\mathbf{q}_{x^*}^n \leq \mathrm{k}_{x^*}^n \tag{B.2}$$
$$\mu_{x^*}^n \mathrm{k}_{x^*}^n \leq \mathbf{q}_{x^*}^n\,, \tag{B.3}$$

where $\mathrm{k}_{x^*}^n \in [0, +\infty]$ is the maximal flow of reference commodity x^* in node n, also called the capacity, and $\mu_{x^*}^n \in [0,1]$ is the minimal load factor of commodity x^* in node n.

For example, a Gas Turbine (GT) can be represented by the following constraints:

$$\alpha_g^{GT} \mathbf{q}_g^{GT} = \beta_{el}^{GT} \mathbf{q}_{el}^{GT} \tag{B.4}$$
$$\alpha_g^{GT} \mathbf{q}_g^{GT} = \beta_{lth}^{GT} \mathbf{q}_{lth}^{GT}\,, \tag{B.5}$$

$$\mathbf{q}_{el}^{GT} \leq \mathrm{k}_{el}^{GT} \tag{B.6}$$
$$\mu_{min}^{GT} \mathrm{k}_{el}^{GT} \leq \mathbf{q}_{el}^{GT}\,, \tag{B.7}$$

where $\mathbf{q}_g^{GT}$ is the flow of gas in the GT in $\mathrm{MWh_{LHV}}$, $\mathbf{q}_{el}$ is the flow of electricity in $\mathrm{MWh_{LHV}}$, $\mathbf{q}_{lth}$ is the low-

temperature (LT) heat flow in $\mathrm{MWh_{LHV}}$, k_{el}^{GT} is the electricity capacity, and μ_{min}^{GT} is the minimal load factor.

Each node is associated with cost functions, and the global objective is to minimize the sum of all these cost functions. All nodes share common cost functions, while some may include additional, node-specific cost functions. The common costs include the installation cost, referred to as CAPital EXpenditure (CAPEX), and operational costs, which are further decomposed into Fixed Operational Maintenance (FOM) costs, which are recurring annual expenses, and Variable Operational Maintenance (VOM) costs, which depend on the flow of commodities through the node at each time step.

Fischer-Tropsch plant. The FT reactor is modeled as a conversion node taking as input CO_2 concentrated gases, hydrogen, and electricity, and outputs FT liquids and HT heat, and LT heat. This FT reactor node is modeled by the following constraints:

$$\alpha_{h_2}^{FT}\mathbf{q}_{h_2}^{FT} = \beta_{ft}^{FT}\mathbf{q}_{ft}^{FT} \tag{B.8}$$
$$\alpha_{el}^{FT}\mathbf{q}_{el}^{FT} = \beta_{ft}^{FT}\mathbf{q}_{ft}^{FT} \tag{B.9}$$
$$\alpha_{co_2}^{FT}\mathbf{q}_{co_2}^{FT} = \beta_{ft}^{FT}\mathbf{q}_{ft}^{FT}\,, \tag{B.10}$$

$$\alpha_{h_2}^{FT}\mathbf{q}_{h_2}^{FT} = \beta_{lth}^{FT}\mathbf{q}_{lth}^{FT} \tag{B.11}$$
$$\alpha_{h_2}^{FT}\mathbf{q}_{h_2}^{FT} = \beta_{hth}^{FT}\mathbf{q}_{hth}^{FT} \tag{B.12}$$
$$\alpha_{el}^{FT}\mathbf{q}_{el}^{FT} = \beta_{lth}^{FT}\mathbf{q}_{lth}^{FT} \tag{B.13}$$
$$\alpha_{el}^{FT}\mathbf{q}_{el}^{FT} = \beta_{hth}^{FT}\mathbf{q}_{hth}^{FT}\,, \tag{B.14}$$

where, $\mathbf{q}_{ft}^{FT}$ is the flow of FT liquids in $\mathrm{MWh_{LHV}}$ in the FT reactor, $\mathbf{q}_{el}^{FT}$ is the flow of electricity in $\mathrm{MWh_{LHV}}$, $\mathbf{q}_{h_2}^{FT}$ is the flow of hydrogen in $\mathrm{MWh_{LHV}}$, $\mathbf{q}_{co_2}^{FT}$ is the flow of CO_2 in tons, $\mathrm{MWh_{LHV}}$,$\mathbf{q}_{lth}^{FT}$ is the flow of LT heat in $\mathrm{MWh_{LHV}}$, and $\mathbf{q}_{hth}^{FT}$ is the flow of HT heat in $\mathrm{MWh_{LHV}}$.

The chemical reactor used in the FT reaction is considered with no flexible operations, and we impose a minimal load factor of 100% modeled by the constraint Equation B.3. Indeed, as explained before in Section 4 , the dynamic rate of the FT process is not yet fully understood, and fluctuations in the production may impact the quality of the products Dieterich et al. (2020). Therefore, to avoid a big gap with real operational conditions, we considered a steady-state rate.

Moreover, the CO_2 inputs into the FT plant node are not totally converted into e-fuel, so this CO_2 is released into the atmosphere and is modeled by the constraint:

$$\mathbf{q}_{co_2}^{FT} = \eta_{co_2}^{FT}\mathbf{q}_{co_2-c}^{FT} + (1-\eta_{co_2}^{FT})\mathbf{q}_{co_2-r}^{FT}\,, \tag{B.15}$$

where $\mathbf{q}_{co_2-c}^{FT}$ is the mass of CO_2 converted into e-fuel in tons, $\mathbf{q}_{co_2-r}^{FT}$ is the mass of CO_2 released in the atmosphere, and $\eta_{CO_2}^{FT} \in [0,1]$ is the carbon efficiency.

The FT node shares the common cost function but includes two additional objective, which are to maximize the profit from the FT liquids and to maximize the CO_2 emission allowances (more details in Figure 3) obtained from each ton of CO_2 converted into e-fuel. These two objectives can be modeled with the following cost function:

$$\psi_{spec}^{FT} = -\mathbf{q}_{ft}^{FT}\cdot\boldsymbol{\phi}_{ft} - \mathbf{q}_{co_2-c}^{FT}\cdot\boldsymbol{\phi}_{co_2-c}\,, \tag{B.16}$$

where ψ_{spec}^{FT} is the node-specific cost function, $\boldsymbol{\phi_{ft}}$ is a time-indexed vector of the selling price per $\mathrm{MWh_{LHV}}$ of the FT liquids, and $\boldsymbol{\phi_{co_2-c}}$ is a time-indexed vector of the selling price of CO_2 emission allowance per ton of CO_2 converted into e-fuel.

Post-combustion carbon capture. The modeling of the PCCC node is similar to Mbenoun et al. (2025); Dachet et al. (2023), but we have modified and added constraints to account for heat exchange flows. This constraint allows the injection of HT waste heat to replace the electricity used to maintain the operating temperature of the PCCC chemical reaction. This behavior can be represented as:

$$\alpha_{hth}^{PCCC}\left(\mathbf{q}_{el-heat}^{PCCC} + \mathbf{q}_{hth}^{PCCC}\right) = \beta_{CO_2}^{PCCC}\mathbf{q}_{CO_2}^{PCCC} \tag{B.17}$$
$$\alpha_{el}^{PCCC}\mathbf{q}_{el}^{PCCC} = \beta_{el-heat}^{PCCC}\mathbf{q}_{el-heat}^{PCCC} \tag{B.18}$$
$$\alpha_{el}^{PCCC}\mathbf{q}_{el}^{PCCC} = \beta_{el-el}^{PCCC}\mathbf{q}_{el-el}^{PCCC}\,, \tag{B.19}$$

where $\mathbf{q}_{el}^{PCCC}$ is the flow of input electricity, $\mathbf{q}_{el-heat}^{PCCC}$ is the electricity used to generate HT heat, $\mathbf{q}_{hth}^{PCCC}$ is the HT heat coming from the waste heat of other assets, $\mathbf{q}_{CO_2}^{PCCC}$ represents the CO_2 captured, and $\mathbf{q}_{el-el}^{PCCC}$ represents the energy needs that can only be met with electricity.

Moreover, we have considered an output flow of the recoverable LT heat modeled by the following constraint:

$$\beta_{lth}^{PCCC}\mathbf{q}_{lth}^{PCCC} = \beta_{co_2}^{PCCC}\mathbf{q}_{co_2}^{PCCC}\,, \tag{B.20}$$

Electrolyzer. The electrolyzers are formulated similarly to Mbenoun et al. (2025); Dachet et al. (2023), but we have introduced a new constraint to model the flow of recoverable LT heat. This constraint is modeled as follows:

$$\alpha_{el}^{EC}\mathbf{q}_{el}^{EC} = \alpha_{lth}^{EC}\mathbf{q}_{lth}^{EC}\,, \tag{B.21}$$

Moreover, the electrolyzers produce O_2 as a by-product of H_2 production. An additional cost function is introduced to model the sale of this oxygen, which can be

formalized as follows:

$$\psi^{EC}_{spec} = -\mathbf{q}^{EC}_{O_2} \cdot \boldsymbol{\phi}_{\boldsymbol{O_2}}\,, \tag{B.22}$$

where ψ^{EC}_{spec} is the node-specific cost function, $\mathbf{q}^{EC}_{O_2}$ is a time-indexed vector of oxygen produced by the electrolyzer in tons, and $\boldsymbol{\phi}_{\boldsymbol{O_2}}$ is a time-indexed vector of oxygen selling prices in euros per ton.

Factory. The factory is modeled with constant output flows, specifically considering only the flow of flue gases in this case study. This flow can be represented by:

$$\mathbf{q}^{F}_{CO2} = \mathbf{1} \cdot \lambda\,, \tag{B.23}$$

where $\mathbf{1}$ is a vector of ones of size T, λ is a constant representing the mean flow of CO_2 of the factory, and $\mathbf{q}^{F}_{\mathrm{CO_2}}$ is the CO_2 mass content in tons of flue gases coming from a factory.

District heating. In our model, we assume that the LT heat generated by all nodes is used as district heating. This district heating is represented by a central node that aggregates the LT heat flows from various model assets. This central node receives multiple LT heat flows from the DEFH assets and outputs a district heat flow without any losses. This process can be expressed as:

$$\sum_{n \in \mathcal{N}} \mathbf{q}^{n}_{lth} = \mathbf{q}^{DHN}_{dh}\,, \tag{B.24}$$

where, $\mathcal{N}$ represents the set of nodes considered, $\mathbf{q}^{n}_{lth}$ denotes the LT heat flow from node n, and $\mathbf{q}^{DHN}_{dh}$ is the district heat flow within the district heating network. Additionally, this node aims to maximize the valorization of LT heat as district heating, which can be modeled with the following cost function:

$$\psi^{DHN}_{spec} = -\mathbf{q}^{DHN}_{dh} \cdot \boldsymbol{\phi}_{dh}\,, \tag{B.25}$$

where ψ^{DHN}_{spec} is the node-specific cost function, $\mathbf{q}^{DHN}_{dh}$ is a time-indexed vector of district heating passing through the district heating network and $\boldsymbol{\phi}_{\boldsymbol{dh}}$ is a time-indexed vector of district heat selling prices in euros per MWh.

Grid. The grid is modeled as a node with only a capacity constraint. The capacity of the installed connection limits the flow of electricity and can be expressed as follows:

$$\mathbf{q}^{G}_{el} \leq \Omega^{G}_{el}\,, \tag{B.26}$$

where $\mathbf{q}^{G}_{el}$ represents the flow of electricity drawn from the grid, and Ω^{G}_{el} denotes the fixed electricity capacity of the grid. As previously explained in Section 4, the grid connection is assumed to be fixed and is not a variable of the model. The CAPEX, FOM and VOM of the grid are not fixed and depend on certain model variables. This cost formulation is derived from Elia (2024). The fixed operational cost of the grid can be formulated as follows:

$$\psi^{G}_{fom} = (\pi_3 + \pi_2) \cdot p^{G}_{yr\text{-}peak} + \pi_1 \sum_{i=0}^{11} p^{G}_{mth\text{-}peak}, \tag{B.27}$$

where the various parameters and variables of this equation are described in Table B.7.

The variable operational cost of the grid can be written as:

$$\psi^{G}_{vom,t} = \psi^{G}_{el\text{-}trans,t} + \psi^{G}_{el\text{-}purchase,t} \tag{B.28}$$

$$\psi^{G}_{vom,t} = (\zeta_1 + \zeta_2) + (\phi_{el\text{-}market,t} + \phi_{el\text{-}margin}), \tag{B.29}$$

where various parameters and variables of this equation are described in Table B.7.

Variable	**Description**	**Value**
ψ^G_{fom}	FOM cost	variable [€]
$\psi^G_{vom,t}$	VOM cost	variable [€]
$q^G_{el,t}$	Electricity drawn from the grid	variable [MWh]
$p^G_{yr-peak}$	Annual peak power demand	variable [GW]
$p^G_{mth-peak}$	Monthly peak power demand	variable [GW]
Parameters	**Description**	**Value**
π_1	Monthly peak	0.2099×10^6 [€/GW]
π_2	Annual peak	5.2958×10^6 [€/GW]
π_3	Available power	4.5060×10^6 [€/GW]
ζ_1	Electricity grid management	0.9195 [€/MWh]
ζ_2	Market integration	0.3706 [€/MWh]
$\phi_{el-market}$	Day-ahead electricity market price	ENTSO-E (2024) [€/MWh]
$\phi_{el-margin}$	Margin of the electricity supplier	10 [€/MWh]

Table B.7: Parameters and variables of the electricity grid operational cost

Appendix C. Calculation

In this section, computation results used throughout the paper are detailed to support the assumptions and numerical values presented in the main analysis. These include large-scale estimations of the impact of DEFHs when integrated into heavy industries, as well as price estimation for synthesized FT liquids based on current fossil fuel market data.

Appendix C.1. DEFH integrated with the cement industry impact calculation

If the concept of DEFH is widely adopted, we can envision a future where every heavy industrial plant has its own DEFH. These hubs would recycle CO_2-rich flue gas, waste heat, or any by-products produced by these plants into e-fuel. Consider the cement industry as an example to illustrate the potential impact of DEFHs. In 2022, the cement industry emitted around 1605 Mt of CO_2 emissions worldwide, accounting for 4.3% of total emissions. If these CO_2 emissions are captured and transformed into Fischer-Tropsch (FT) liquids (e-kerosene, e-diesel, and e-naphtha) with a CO_2 efficiency of 72%, then 1123.5 Mt of CO_2 are converted into 370 Mt of FT liquids (4673 TWh). Assuming that 60% by mass of the FT liquids is e-kerosene, this represents 2504 TWh of e-kerosene, or 66.42% of the commercial aviation fuel consumption in 2022 (3773 TWh of fuel). This computation is detailed below.

Our computations are based on a DEFH composed of a factory equipped with Post-Combustion Carbon Capture (PCCC) to capture CO_2 from CO_2-rich flue gas and then send it to the FT plant to synthesize FT liquids with an input of hydrogen and electricity. The PCCC technology considered here has a 90% capture rate, and the FT plant is considered to have 80% CO_2 efficiency, requiring 3.9 tons of CO_2 to synthesize 1 ton of FT liquids. First, the mass of FT liquids produced is computed as follows:

$$m_{FT} = \frac{m_{CO2} \cdot \eta_{PCCC}}{3.9} \tag{C.1}$$

$$370[\text{Mt}] = \frac{1123.5[\text{Mt}] \cdot 0.72}{3.9}, \tag{C.2}$$

where m_{CO2} is the mass of CO_2 released by the factory, η_{PCCC} is the capture rate of PCCC, 3.9 is the conversion mass ratio of CO_2 to FT liquids, and m_{FT} is the mass of FT liquids.

Second, to convert the mass of FT liquids into TWh, we use the following formula:

$$E_{kero} = m_{FT} \cdot \beta_{kero} \tag{C.3}$$

$$2504_{[\text{TWh}]} = (370_{[\text{Mt}]} \cdot 0.6) \cdot 11.277_{[\text{kWh/kg}]}\,, \tag{C.4}$$

where β_{kero} is the energy density per kilogram of kerosene (11.277 kWh_{LHV}) and E_{kero} is the energy of kerosene produced.

Appendix C.2. FT liquids actual gross market price

To determine a relevant price for the FT liquids, we assume a mass distribution of 60% kerosene, 20% diesel, and 20% naphtha. Given the low value of naphtha, its price is neglected. We then assume that for each MWh_{LHV} of FT liquids, 79.3 kg of FT liquids are obtained (see Danish-Energy-Agency (2024) for more details). This results in 47.58 kg of kerosene (density: 0.82 kg/L) and 15.86 kg of diesel (density: 0.85 kg/L). Converting these masses to volumes yields approximately 58 liters of kerosene and 18.66 liters of diesel. The price ϕ_{ft} is computed as follows:

$$\phi_{ft} = V_{kerosene} \cdot \phi_{kerosene} + V_{diesel} \cdot \phi_{diesel}, \tag{C.5}$$

$$66_{[€/\text{MWh}]} \approx 58_{[l]} \cdot 0.96_{[€/l]} + 18.66_{[\text{l}]} \cdot 0.57_{[€/l]}, \tag{C.6}$$

where, $V_{kerosene}$ and V_{diesel} represent the volumes of kerosene and diesel, respectively, for one MWh of FT liquids, $\phi_{kerosene}$ and ϕ_{diesel} are the respective prices (in €/L) of kerosene and diesel in Belgium according to GlobalPetrolPrices.com (2025) and EnergiaFed (2025). Rounding the calculation result, we obtain a price of approximately 66 €/MWh_{LHV} for the fossil fuel equivalent of FT liquids.

Appendix D. Assets parameters

This section presents the economic and technical parameters used in the LP model of our case study DEFH introduced in Section 3. All values are primarily sourced from Danish-Energy-Agency (2024) unless stated otherwise. The economic parameters of the assets are presented in Table D.8 and the technical parameters are presented in Table D.9.

Unit	CAPEX	FOM	VOM	Liftetime [years]
Wind Onshore	1.15 [M€/MW]	0.16663 [M€/MW-yr]	0.00002 [M€/MWh]	30
PV Tracker	0.45 [M€/MW]	0.0104 [M€/MW-yr]	0.0 [M€/MWh]	40
PV	0.38 [M€/MW]	0.0095 [M€/MW-yr]	0.0 [M€/MWh]	40
Grid	0.00154 [M€/MW]	Appendix B.2	Appendix B.2	-
PEMEC	0.950 [M€/MW]	0.0475 [M€/MW-yr]	0.002 [M€/MWh]	25
AEC	0.875 [M€/MW]	0.04375 [M€/MW-yr]	0.004 [M€/MWh]	25
FT reactor	1.701 [M€/MW]	0.085 [M€/MW-yr]	0.000045 [M€/MWh]	25
DAC	2.7 [M€/(tCO_2/h)]	0.10 [M€/(tCO_2/h)]	0.00005 [M€/tCO_2]	30
PCCC	2.5 [M€/(tCO_2/h)]	0.08 [M€/(tCO_2/h)]	0.00002 [M€/tCO_2]	25
CO_2 tank	0.0038 [M€/tCO_2]	0.000114 [M€/tCO_2-yr]	-	25
CO_2 liquefaction	1.33 [M€/(tCO_2/h)]	0.05 [M€/(tCO_2/h)-yr]	-	20
H_2 tank	0.048 [M€/MWh]	0.00532 [M€/MW-yr]	-	30
NaS Battery	0.2445 [M€/MWh]	0.00367 [M€/MWh-yr]	0.00002 [M€/MWh]	24
Li-ion battery	0.66 [M€/MWh]	0.00057 [M€/MWh-yr]	0.00002 [M€/MWh]	25

Table D.8: Economic parameters of assets. These parameters are based on Danish-Energy-Agency (2024) except for the grid, which is based on Elia (2024).

Unit	Parameters	Value
PEMEC	minimal load factor [%]	5
	efficiency[%]	74.7
	recoverable LT heat [%]	26.5
AEC	minimal load factor [%]	30
	efficiency[%]	81.5
	recoverable LT heat [%]	20.6
FT reactor	minimal load factor [%]	100
	efficiency[%]	70
	recoverable HT heat [%]	20
	Carbon efficiency [%]	80
DAC	minimal load factor [%]	0
	energy input [MWh/tCO_2]	1.385
	recoverable LT heat [%]	0.296
PCCC	minimal load factor [%]	0
	energy input [MWh/tCO_2]	0.742
	recoverable LT heat [%]	1.54
	Carbon efficiency [%]	90
CO_2 tank	round-trip efficiency [%]	100
CO_2 liquefaction	round-trip efficiency [%]	100
	maximum charge rate [tCO_2/h]	1
	electricity input [MWh/tCO_2]	0.129
H_2 tank	round-trip efficiency [%]	89
	maximum charge rate [MW_{H_2}]	0.09
	electricity input [MWh_{el}/MWh_{H_2}]	0.01
NaS Battery	round-trip efficiency [%]	85
	maximum charge rate [MW/MWh]	0.1667
	maximum discharge rate [MW/MWh]	0.1667
Li-ion battery	round-trip efficiency [%]	96
	maximum charge rate [MW/MWh]	3
	maximum discharge rate [MW/MWh]	0.5

Table D.9: Technical parameters of assets. The recoverable LT and HT heat is expressed in a percentage of total energy input [MWh/MWh]. These parameters are based on Danish-Energy-Agency (2024).